Tetrahedron Vol. 46, No. 8, pp. 2761-2772, 1990
Printed in Great Britain

0040-4020/90 $3.00+.00

DYNAMIC STEREOCHEMISTRY OF MOLECULAR GEARS. 9-BENZYLTRIPTYCENE AND 9-PHENOXYTRIPTYCENE, STUDIED BY ^{13}C DYNAMIC NMR SPECTROSCOPY AND MOLECULAR MECHANICS CALCULATIONS

Gaku Yamamoto
Department of Chemistry, Faculty of Science,
The University of Tokyo, Bunkyo-ku, Tokyo 113, Japan
(*Received in Japan* 22 *December* 1989)

Abstract: The ^{13}C dynamic NMR and molecular mechanics studies show that gear rotational motion is the most favorable process in 9-phenoxytriptycene, while isolated rotation of the phenyl group corresponding to the slippage of the gear is the lowest energy process in 9-benzyltriptycene.

Correlated internal rotation of two or more bonds in a molecule is an interesting topic in studies of dynamic stereochemistry of organic molecules. Dynamic behavior of compounds in which two or more alkyl groups are attached geminally or vicinally to a planar framework has been extensively studied.[1] In propeller-shaped molecules in which two or three aromatic rings are bonded to a common atomic center, correlated rotation of the aromatic rings has been observed by dynamic NMR spectroscopy and in some cases residual isomerism has been realized.[2,3] While aromatic rings serve as rigid two-fold rotors in these compounds, the 9-triptycyl group has been shown to behave as a rigid three-fold rotor with an extremely high rotational barrier.[4] This finding has lead to the use of the 9-triptycyl group as a building block of stereodynamically interesting molecules. Stable dynamic molecular gears have been realized in Tp_2X compounds (**1**), in which two 9-triptycyl (Tp) groups are attached to a central atom X.[3,5]

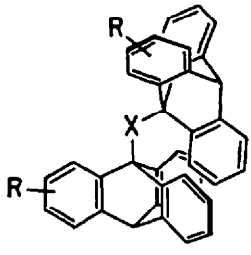

1

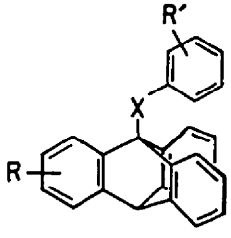

2

We have studied the stereodynamics of another interesting group of triptycene-derived compounds, 9-(phenyl-X)triptycene derivatives (**2**) where X is CH_2[6,7] or O,[7,8] by ^1H dynamic NMR spectroscopy. These molecules are regarded as molecular bevel gears consisting of a

two-toothed wheel and a three-toothed one. Compounds we have studied so far are substituted derivatives of 9-benzyltriptycene (**3**) and 9-phenoxytriptycene (**4**), and the parent compounds have been left to be studied. The reason for this is simply that it is difficult to obtain quantitative information on the stereodynamics of these compounds by ^1H NMR spectra. Recent availability of high-field NMR spectrometers prompted us to investigate the stereodynamics of 3 and 4 by ^{13}C dynamic NMR spectroscopy. We also carried out molecular mechanics calculations in order to supplement the experimental results.

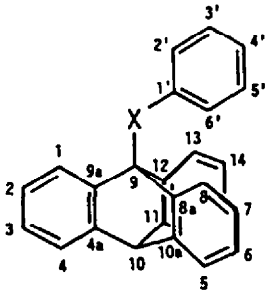

3 : X = CH_2

4 : X = O

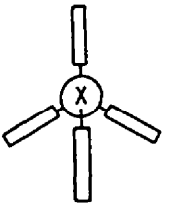

5

In the ground states the molecules are assumed to exist in a conformation in which the plane of the phenyl (Ph) group is nearly coplanar with the Tp-X bond, bisecting the "notch" made of two benzene rings of the triptycene skeleton as shown by the Newman projection along the Tp-X bond axis (**5**). As for the molecular motions exhibited by these molecules, two fundamental processes are to be considered as revealed by inspection of molecular models. One is gear rotation (GR) in which concomitant rotation of the Tp-X bond by 120° and the Ph-X bond by 180° occurs in a disrotatory fashion and the transition state for this process is represented by the Newman projection formula **6**. The other is isolated rotation (IR) of the Ph-X bond which takes place without concomitant Tp-X rotation by way of the transition state shown by **7**. A third process, isolated rotation of the Tp-X bond (IR') may be neglected because the plausible transition state **8** is highly unlikely. Therefore, the rotation about the Tp-X bond takes place only by the GR process, always accompanied by the rotation of the Ph-X bond, while the rotation about the Ph-X bond occurs by either of the GR or IR process.

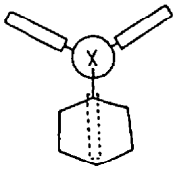

6
GR

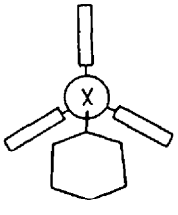

7
IR

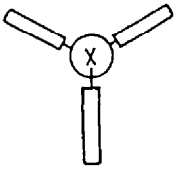

8
IR'

Results and Discussion

^{1}H NMR Spectra. The ^{1}H NMR spectrum of the aromatic protons of 9-benzyltriptycene (3) in CD_2Cl_2 at 25 °C shows a rather simple pattern reflecting rapid internal motions (Fig. 1, top). On lowering the temperature, the signals broaden and further split. At -80 °C, the Tp-C rotation is slow on the NMR time scale and the aromatic protons of the triptycene moiety appear as considerably sharp signals, while those of the Ph group except for 4'-H can hardly be recognized because of extensive broadening. At -95 °C the Ph-C rotation slows down though not completely frozen (Fig. 1).

The spectral pattern at the lowest temperature is compatible with the conformation shown by the Newman projection 5. The signals are assigned as shown in Fig. 1, judging from the relative intensities, splitting patterns, and ring-current effects of the benzene rings. The very large chemical shift difference between the 2'-H and 6'-H signals (1.05

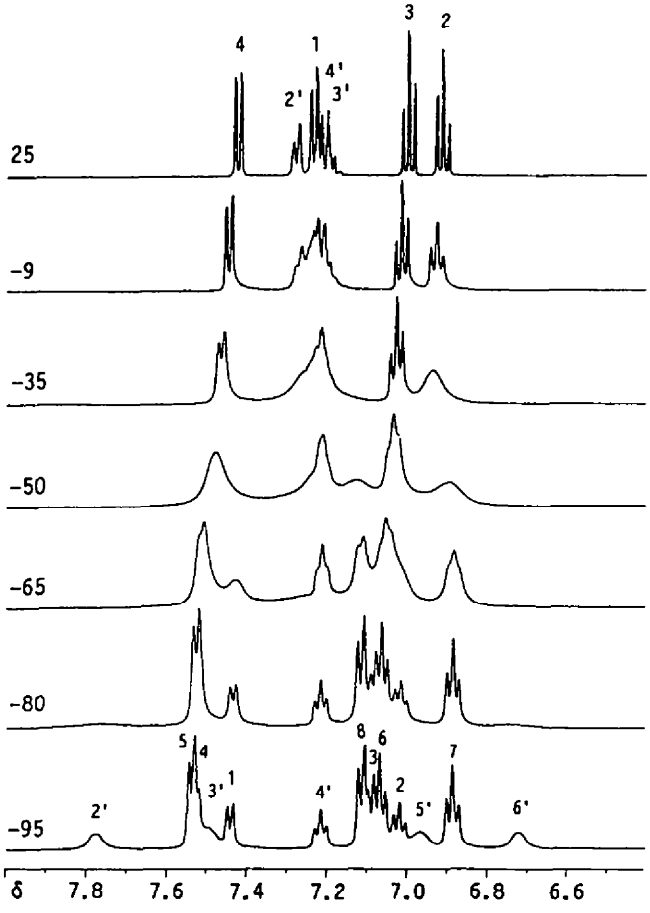

Fig. 1. The aromatic proton signals of 3 at various temperatures (°C) in CD_2Cl_2.

ppm) is remarkable. The 6'-proton is strongly shielded by the ring-current effect of the flanking benzene rings of the Tp moiety and weakly deshielded by the remote benzene ring, while the 2'-proton is weakly deshielded by all of the three Tp-benzene rings. Similarly the 8/13-H signal appears at higher field than 1-H by 0.32 ppm reflecting the differential ring-current effect by the phenyl group. A rough estimate using the Johnson-Bovey diagram[9] and the geometry obtained by the BIGSTRN-3 calculation described below predicts the chemical shift difference between 2'-H and 6'-H of ca. 1.1 ppm and that between 1-H and 8/13-H of ca. 0.6 ppm in good agreement with the experimental results.

The variable temperature ^1H NMR spectra qualitatively indicate that the Tp-C rotation takes place at a higher temperature range and thus has a higher energy barrier than the Ph-C rotation, but do not afford quantitative information about the kinetic parameters.

The ^1H spectrum of 9-phenoxytriptycene (**4**) in CD_2Cl_2 at 25 °C reflects the rapid internal motions. The aromatic proton signals are considerably broadened but show no further splitting at -95 °C, suggesting still fast motions at this temperature.

^{13}C NMR Spectra. The completely ^1H-decoupled ^{13}C NMR spectrum of 3 at 25 °C reflects the fast internal motions of the molecule and comprises ten aromatic carbon signals together with three aliphatic carbon signals (Fig. 2, top). Two peaks assignable to 1/8/13-C and 9a/8a/12-C are considerably broadened because of the large chemical shift differences between the diastereotopic carbons in the conformationally frozen state.

The ^{13}C spectrum of **4** at 25 °C is composed of twelve sharp peaks, ten aromatic and two aliphatic, suggesting very fast internal motions (Fig. 3, top).

Assignments of the chemical shifts are made by reference to the ^1H-coupled and selectively ^1H-decoupled spectra. The results are compiled in Table 1. In ^1H-coupled spectra, aromatic carbon signals are typically characterized by a large $^1J_{CH}$ of about 160 Hz, if a proton is attached to the carbon in question, and $^3J_{CH}$ couplings of about 7 Hz with aromatic proton(s) meta to the carbon, $^2J_{CH}$ and $^4J_{CH}$ being usually unresolved.[10] In selective ^1H-decoupling experiments, $^3J_{CH}$ was decoupled by weak irradiation of a particular aromatic proton signal, because irradiation with high power caused concomitant irradiation of nearby proton signals and thus did not afford unambiguous decoupling information. The data in Table 1 were obtained in $CDCl_3$ and the chemical shifts in CD_2Cl_2 were easily assigned without ambiguity, although all the peaks appeared systematically at lower field by 0.2-0.7 ppm in CD_2Cl_2 than in $CDCl_3$.

On lowering the temperature, all the aromatic carbon signals in compound 3 except for those of the ipso- and p-carbons of the phenyl group gradually broaden and each of them splits into two peaks. A nearly frozen spectrum is obtained at -102 °C. The aromatic carbons of the triptycene skeleton give rise to six pairs of peaks with an intensity ratio of 2:1 while the o- and m-carbons of the phenyl group afford two equally intense peaks, respectively (Fig. 2 and Table 2). These spectral features are compatible with the ground state conformation discussed above.

The low temperature ^{13}C spectra of 3 reveal several intriguing features. The 1-C

Table 1. ^{13}C NMR data of 9-benzyltriptycene (**3**) and 9-phenoxytriptycene (**4**) (^{1}H-Coupled, $CDCl_3$, 25 °C)

3			4		
δ	coupling/Hz[a)]	carbon	δ	coupling/Hz[a)]	carbon
33.09	t 125.1, t 4.0	CH_2	53.36	d 141.7, q 4.0	10
52.25	br m	9	85.67	br	9
54.55	d 140.7, q 4.0	10	118.35	d 162.8, m	2'
123.33	d 158.7, d 8.0, d 4.0, m	4	120.98	d 160.5, t 7.8	4'
123.47	br d 158.8, d 7.5	1	122.68	d 162.2, d 7.9	1
124.52	d 159.8, d 7.3	2	123.20	d 159.3, d 7.5, d 4.0, m	4
124.96	d 159.8, d 7.3	3	124.57	d 160.5, d 7.3	2
125.63	d 160.3, t 7.2	4'	125.40	d 159.9, d 7.3	3
127.69	d 159.5, d 7.2	3'	128.60	d 161.0, d 7.2, m	3'
130.61	d 157.6, t 7.2, t 3.4	2'	143.29	q 6.6	9a
137.16	quint 6.8	1'	143.62	t 7.0, d 3.5	4a
145.65	br	9a	155.83	br t 9.8	1'
146.64	t 7.3, d 3.7	4a			

a) d:doublet, t:triplet, q:quartet, quint:quintet, m: multiplet, br:broad; coupling constants are reliable to ±0.6 Hz.

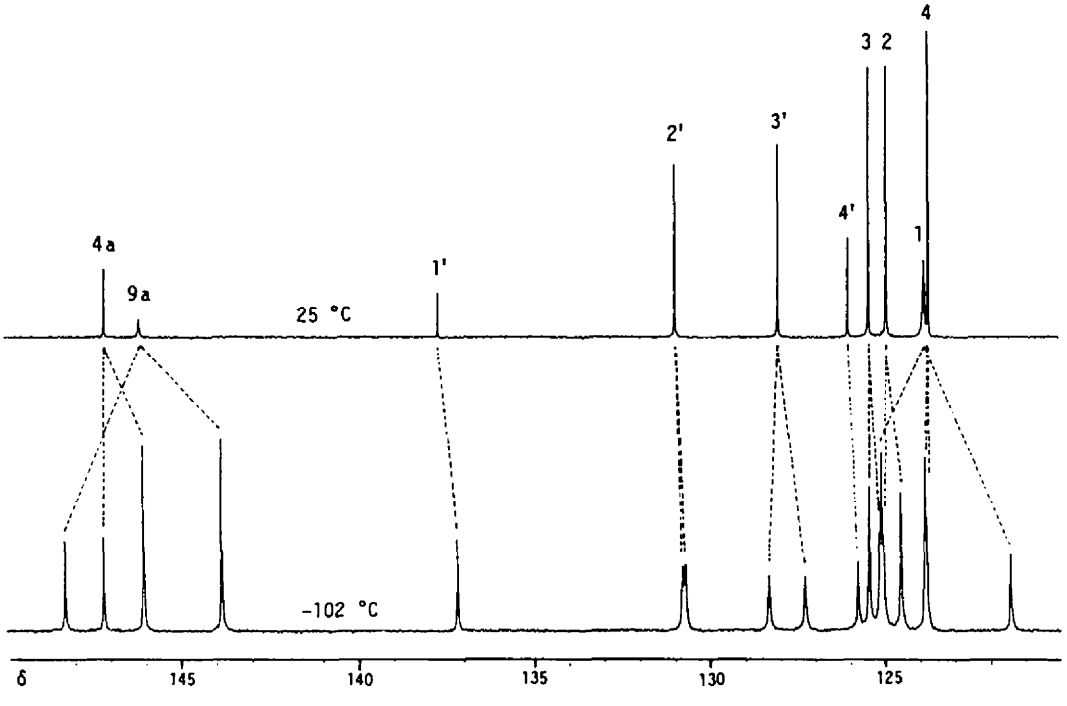

Fig. 2. ^{13}C NMR spectra of the aromatic carbons of **3** at 25 and -102 °C.

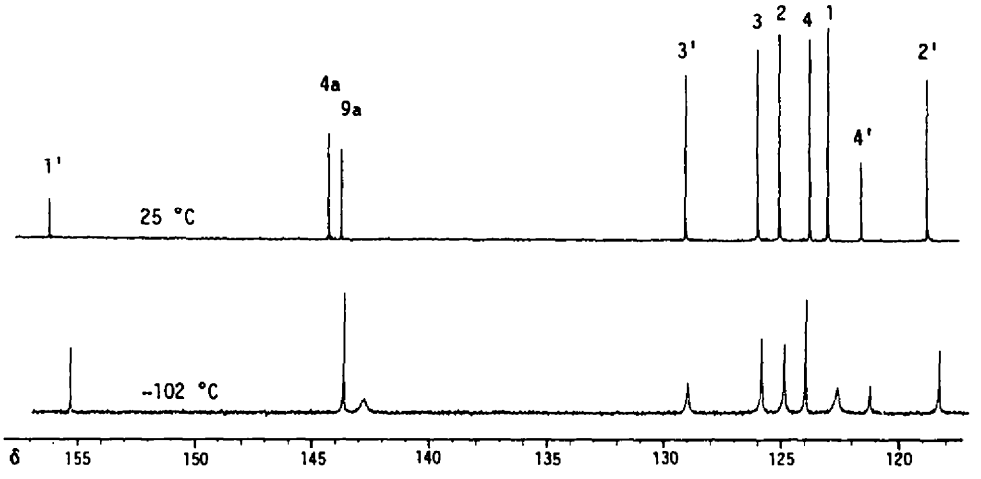

Fig. 3. ^{13}C NMR spectra of the aromatic carbons of **4** at 25 and -102 °C.

Table 2. ^{13}C chemical shifts (δ) of 9-benzyltriptycene (**3**) and 9-phenoxytriptycene (**4**) at 25 and -102 °C in CD_2Cl_2

Carbon[a]	3				4	
	25°C	-102°C	ppm[b]	Hz[b]	25°C	-102°C
1 8,13	123.84	121.43 125.10	3.67	461.5	122.90	122.62
2 7,14	124.91	125.04 124.55	0.49	62.0	124.97	124.89
3 6,15	125.42	125.16 125.46	0.30	38.5	125.91	125.86
4 5,16	123.72	123.81 123.86	0.05	5.9	123.68	123.98
4a 10a,11	147.11	147.21 146.09	1.12	141.4	144.29	143.67
9a 8a,12	146.14	148.32 143.89	4.43	557.7	143.73	142.76
9	52.70	51.96			86.03	85.22
10	54.81	53.47			53.59	52.31
CH_2	33.35	32.48				
1'	137.67	137.20			156.21	155.30
2' 6'	130.95	{130.79[c] 130.70	0.09	10.8	118.66	118.32
3' 5'	128.03	{128.34[c] 127.31	1.03	129.2	129.01	128.99
4'	126.02	125.79			121.47	121.24

a) Numbers are as shown in the formula **3**/**4**. b) Chemical shift difference between the diastereotopic carbons at -102 °C.
c) Assignments are not made.

signal appears at higher field than the 8/13-C signal by 3.67 ppm, in sharp contrast with the behavior of the corresponding proton signals. On the contrary, the 9a-carbon gives its signal at lower field than the 8a/12-carbons by 4.43 ppm. These facts suggest that the ring-current effect is less significant in ^{13}C spectra. Also interesting is that the chemical shift difference between 3'-C and 5'-C of the Ph group (1.03 ppm) is far larger than that between 2'-C and 6'-C (0.09 ppm). Electron distribution perturbed by interactions among the aromatic rings may be responsible for these phenomena.

In 9-phenoxytriptycene (**4**), the internal motions are still fast on the NMR time scale even at -111 °C, the lowest attainable temperature, although some of the peaks are considerably broadened (Fig. 3, bottom).

Lineshape Analysis. The lineshapes of the signal due to the 4a/10a/11-carbons of the Tp moiety in **3** were analyzed using the DNMR3 program[11] at five temperatures between -34 and -65 °C and the best-fit rate constants were obtained (Fig. 4). Similarly, the lineshapes of the 3'/5'-carbon signals of the Ph group were analyzed at six temperatures between -65 and -96 °C (Fig. 5). The kinetic parameters obtained therefrom using the least squares method are shown in Table 3. The calculated spectra at -72 and -96 °C in Fig. 4 and those at -59 and -102 °C in Fig. 5 are obtained using the rate constants calculated from the data in Table 3.

Diastereotopicity of the aromatic carbons of the triptycene skeleton is ascribed to slow rotation of the Tp-X bond. As we assume that rotation of the Tp-X bond is always accompanied by rotation of the Ph-X bond, the lineshapes of the triptycene carbon signals give the rate constants of gear rotation (GR). Meanwhile, rotation of the Ph-X bond occurs either concomitantly with that of the Tp-X bond (GR) or independently of it (IR). Therefore the rate constants obtained from the lineshapes of the phenyl carbons are the sum of k_{GR} and k_{IR}.

Table 3 indicates that both the enthalpy and the free energy of activation obtained from the Tp-carbon analysis are ca. 1.5 kcal mol^{-1} higher than those obtained from the Ph-carbon analysis. At -65 °C, the rate constant for the Ph-C rotation is calculated to be 1300 s^{-1} and that for the Tp-C rotation to be 25 s^{-1}, about one fiftieth of the former. Therefore, the contribution of the GR process to the Ph-C rotation is negligible and the kinetic parameters from the Ph-carbon analysis are regarded to represent those for the IR

Table 3. Kinetic parameters from dynamic NMR of **3**

Obs'd Carbon	Temp Range[a] °C	$\Delta H^{\ddagger}$ kcal mol^{-1}	$\Delta S^{\ddagger}$ cal mol^{-1} K^{-1}	$\Delta G^{\ddagger}_{250}$ kcal mol^{-1}	k at -65°C s^{-1}	Process
4a/10a/11	-34~-65	9.96 ±0.35	-3.5 ±1.6	10.8_4	25	GR
3'/5'	-65~-96	8.53 ±0.04	-2.6 ±0.2	9.1_8	1300	IR (+GR)

a) The temperature range in which DNMR simulations were made. See Figs. 4 and 5.

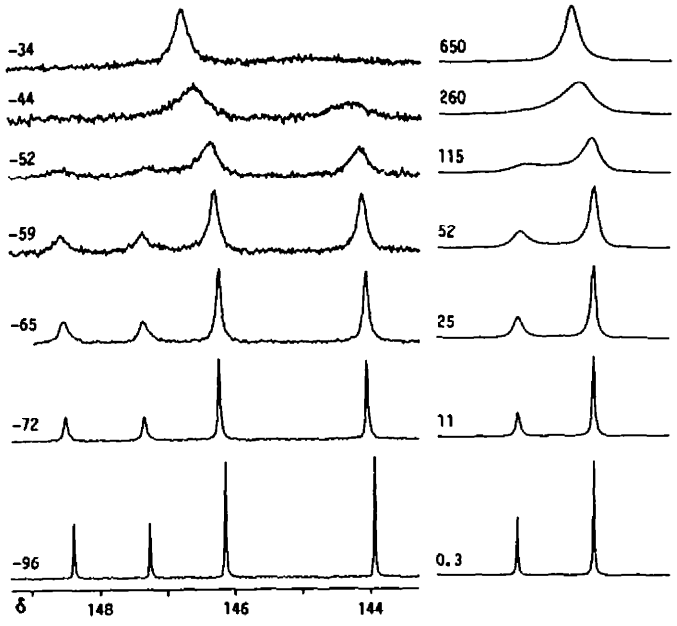

Fig. 4. The observed spectra (left, inside) of the 4a/10a/11-carbons of 3 at various temperatures (°C) and the calculated spectra (right) with the best-fit rate constants (s^{-1}).

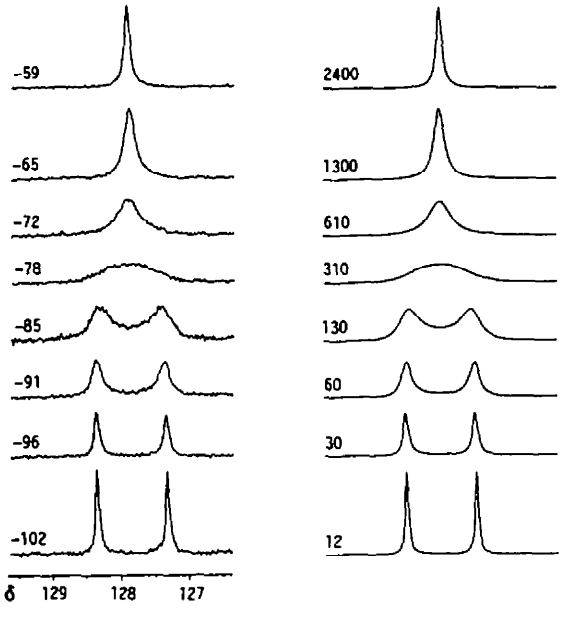

Fig. 5. The observed spectra (left) of the 3'/5'-carbons of 3 at various temperatures (°C) and the calculated spectra (right) with the best-fit rate constants (s^{-1}).

process.

Kinetic parameters for compound **4** can not be determined because the slow-exchange-limit spectra have not been obtained. A rough estimate of the rate constants is however made as follows. The halfwidth of the signal assigned to 3'/5'-C of the phenyl group is 13 Hz at -102 °C and 33 Hz at -111 °C. If the chemical shift difference between 3'-C and 5'-C is assumed to be 130 Hz, as observed in **3**, rate constants for the Ph-O rotation are estimated to be ca. 2700 and 900 s^{-1} at -102 and -111 °C, respectively. These values correspond to the free energy of activation of ca. 7.1 kcal mol^{-1}. In the meantime, the halfwidth of the 4a/10a/11-C signal is 37 Hz at -102 °C and ca. 100 Hz at -111 °C. With the chemical shift difference of 550 Hz, the value found for the corresponding carbons in **3**, the rate constants for the Tp-O rotation are estimated to be 9000 s^{-1} at -102 °C and 2000 s^{-1} at -111 °C. These estimates are inconsistent because the rate constant for the Tp-O rotation should not be larger than that for the Ph-O rotation according to the discussion given above. The actual chemical shift differences in **4** might thus be considerably different from those of the corresponding carbons in **3**. Anyway, the search suggested that the Tp-O rotation and the Ph-O rotation have almost the same energy barriers of ca. 7 kcal mol^{-1}.

Molecular Mechanics Calculations. For compound **3**, detailed molecular mechanics study has been made by Mislow and his coworkers[12] using the BIGSTRN-3 program[13] with the MM2 force field and full-matrix Newton-Raphson optimization procedure. Employing the same program, we performed the calculations on both **3** and **4** and obtained the energies and geometries of the ground states (GS) and the transition states (TS) for the GR, IR and IR' processes (Table 4). All of these stationary states have C_s symmetry. The GR transition state **7** and the IR one **8** are calculated as saddle points in the energy surface with one negative eigenvalue of the matrix of analytical second derivatives, while the structures assumed as the IR' transition state **9** correspond to a double partial maximum with two negative eigenvalues.

As for compound **3**, our results completely reproduced those by Mislow's group.[12] The calculated energy barriers are however considerably larger than the experimentally

Table 4. Results of BIGSTRN-3 calculations (kcal mol^{-1})

Stationary Point	**3**				**4**			
	E_s a)	Rel Energy a)	E_s b)	Rel Energy b)	E_s a)	Rel Energy a)	E_s b)	Rel Energy b)
GS	12.60	0	37.82	0	14.31	0	36.46	0
TS(GR)	26.57	13.97	49.74	11.91	22.39	8.08	44.26	7.79
TS(IR)	24.05	11.45	48.13	10.30	30.18	15.87	51.37	14.91
TS(IR')	52.10	39.50	73.16	35.34	49.47	35.16	69.62	33.16

a) Using the original MM2 force field. b) Using the modified MM2 force field emulating MM3. See text.

obtained enthalpies of activation. Especially the GR barrier is 4 kcal mol^{-1} higher than the observed one. It has been pointed out[12] that because of the intrinsic nature of the force field used the repulsive interaction between a benzene ring and a hydrogen located closely above the benzene plane tends to be overestimated. The overestimation of the GR barrier may at least partly be ascribed to this factor. Recently a new force field (MM3) has been developed by Allinger and his co-workers,[14] which seems to overcome this deficiency to some extent, introducing bond dipoles for $C(sp^2)$–H and $C(sp^2)$–$C(sp^3)$ bonds and modifying some of the van der Waals parameters. As the program is not yet available to us, we performed BIGSTRN-3 calculations with incorporation of these modifications into the original MM2 force field. The results obtained show considerable improvements as shown in Table 4. Although the barriers are still somewhat larger than the observed ones, the barrier difference between GR and IR of ca. 1.5 kcal mol^{-1} are well reproduced.

As for compound **4**, the calculations clearly show that the IR barrier is far higher than the GR one. This suggests that GR is the only process observed, and that the Tp–O rotation and the Ph–O rotation have the same energy barrier corresponding to GR. This supports the experimental estimation described above, and the calculated GR barrier of 7.8 kcal mol^{-1} agrees well with the estimated value, if the overestimation mentioned above is taken into account.

In conclusion, 9-phenoxytriptycene (**4**) behaves as a tightly meshed dynamic bevel gear with correlated disrotation of the Tp–O and Ph–O bonds as the lowest energy process, while isolated rotation corresponding to "slippage" of the gear occurs preferably in 9-benzyltriptycene (**3**). The differential behavior of **3** and **4** is understood in terms of two factors as discussed before,[8] i.e. bond lengths of C–C vs. C–O and valencies of C vs. O. There exist three pairs of eclipsing interactions in the GR transition state of **3** (**6**: $X=CH_2$), while only one pair in the GR transition state of **4** (**6**: X=O) because the steric interaction involving lone-pair electrons on oxygen may be neglected. This valency effect may be the main factor for the higher GR barrier in **3** than in **4**. In the IR transition states (**7**), the largest steric interactions take place between the o-hydrogens of the Ph group and the flanking peri-hydrogens of the Tp moiety. Compound **4** with shorter C–O bonds might suffer from larger steric congestion than **3** with longer C–C bonds, resulting in the higher IR barrier in **4** than in **3**.

In Tp_2X compounds **1**, the differences in the C–X–C bond angles and their bending force constants have been suggested to significantly affect the difference in the energy barriers to gear slippage between **1**($X=CH_2$) and **1**(X=O).[5,15] In contrast, careful examination of the present BIGSTRN-3 results reveals that the factor of bond bending does not significantly contribute to the differential behavior of **3** and **4**.

Experimental

^1H and ^{13}C NMR spectra were obtained on a Bruker AM-500 spectrometer at 500.17 and 125.76 MHz, respectively, in the pulse FT mode. The digital resolution was 0.305 and

0.610 Hz/point for the ^1H and ^{13}C spectra, respectively. Tetramethylsilane was used as the internal standard. In the variable temperature ^{13}C NMR experiments, a solution of ca. 10 mg of **3** or **4** in 0.5 ml of CD_2Cl_2 was used and 800 to 1600 FID's were collected at each temperature under completely ^1H-decoupled conditions using the composite pulse decoupling (CPD) sequence. Temperatures were calibrated with a methanol sample (4% CH_3OH in CD_3OD) according to the Bruker operation manual and were reliable to ±1.0 °C.

9-Benzyltriptycene (**3**). To a boiling solution of 537 mg (2.0 mmol) of 9-benzylanthracene[16] in 30 ml of acetone was added from separate dropping funnels a solution of 1.37 g (10.0 mmol) of anthranilic acid in 50 ml of acetone and a solution of 2.5 ml (ca. 20 mmol) of isopentyl nitrite in 50 ml of acetone during the course of 2 h and the mixture was heated under reflux for further 1 h. The reaction mixture was evaporated and the residue was chromatographed through an alumina column with hexane as the eluent. Recrystallization of the eluted product from hexane-dichloromethane gave 420 mg (61%) of **3** as colorless crystals, mp 231-232 °C. Found :C, 94.10; H, 6.15%. Calcd for $C_{27}H_{20}$: C, 94.15; H, 5.85%. ^1H NMR ($CDCl_3$, 25 °C): δ 4.481 (2H, s, CH_2), 5.436 (1H, s, 10-H), 6.891 (3H, dt, J=1.2 and 7.5 Hz, 2/7/14-H), 6.971 (3H, dt, J=1.0 and 7.5 Hz, 3/6/15-H), 7.17-7.25 (6H, m, 1/8/13-H, 3'/5'-H, and 4'-H), 7.299 (2H, d, J=7.0 Hz, 2'/6'-H), 7.399 (3H, dd, J=1.0 and 7.3 Hz, 4/5/16-H). Assignments of ^1H chemical shifts were unambiguously made on the basis of NOE (irradiation of the 10-H signal enhanced the 4/5/16-H signal) and homonuclear decoupling experiments.

9-Phenoxytriptycene (**4**). The same procedure as for the synthesis of **3** was employed using 540 mg (2.0 mmol) of 9-phenoxyanthracene[17] instead of 9-benzylanthracene. After the reaction was complete, the solvent was evaporated and the residue was chromatographed through an alumina column with hexane-dichloromethane as the eluent, which gave a mixture containing about 30% of unreacted 9-phenoxyanthracene. The mixture was heated under reflux with 1.0 g of maleic anhydride in 15 ml of acetonitrile for 24 h and chromatographed through alumina with hexane-dichloromethane as the eluent. Recrystallization of the eluate from hexane-dichloromethane gave 274 mg (40%) of **4** as colorless crystals, mp 267-268 °C. Found: C, 90.10; H, 5.44%. Calcd for $C_{26}H_{18}O$: C, 90.14; H, 5.24%. ^1H NMR ($CDCl_3$, 25 °C): δ 5.402 (1H, s, 10-H), 6.942 (3H, dt, J=1.2 and 7.5 Hz, 2/7/14-H), 6.995 (3H, dt, J=1.3 and 7.3 Hz, 3/6/15-H), 6.98-7.03 (1H, m, 4'-H), 7.08-7.12 (2H, m, 2'/6'-H), 7.22-7.28 (2H, m, 3'/5'-H), 7.397 (3H, dd, J=1.0 and 7.3 Hz, 4/5/16-H), 7.427 (3H, dd, J=1.1 and 7.4 Hz, 1/8/13-H).

Molecular Mechanics Calculations. The calculations were performed on a Hitac M-682 computer system at the Computer Center of the University of Tokyo using the BIGSTRN-3 program[13] with the MM2 force field and full-matrix Newton-Raphson procedure. A torsional parameter V_3 of 0.34 kcal mol^{-1} for $C(sp^2)$-$C(sp^3)$-O-$C(sp^2)$ was added to the original force field. In the calculations where the MM3 force field was emulated, the bond moments of 0.6 and 0.9 D were assigned to the $C(sp^2)$-H and $C(sp^2)$-$C(sp^3)$ bonds, respectively, the sp^2-carbon being the negative end of the dipole in each case. In addition, some of the van der Waals parameters were modified as follows: r=1.96 Å, ε=0.056 for $C(sp^2)$; r=1.62 Å,

ϵ=0.020 for H.

Acknowledgment. The present work was supported by a Grant-in-Aid for Scientific Research on Priority Areas (No. 01648607) from the Ministry of Education, Science and Culture of Japan.

References

1. Berg, U.; Liljefors, T.; Roussel, C.; Sandstrom, J. Acc. Chem. Res. **1985**, 18, 80–86.
2. Gust, D.; Mislow, K. J. Am. Chem. Soc. **1973**, 95, 1535–1547. Mislow, K. Acc. Chem. Res. **1976**, 9, 26–33.
3. Mislow, K. Chemtracts-Org. Chem. **1989**, 2, 151–174.
4. Ōki, M. Angew. Chem., Int. Ed. Engl. **1976**, 15, 87–93; Top. Stereochem. **1983**, 14, 1–81.
5. Iwamura, H.; Mislow, K. Acc. Chem. Res. **1988**, 21, 175–182.
6. a) Yamamoto, G.; Ōki, M. Bull. Chem. Soc. Jpn. **1981**, 54, 473–480. b) Yamamoto, G.; Ōki, M. ibid. **1981**, 54, 481–487. c) Yamamoto, G.; Ōki, M. J. Org. Chem. **1983**, 48, 1233–1236. d) Yamamoto, G. Bull. Chem. Soc. Jpn. **1989**, 62, 4058–4060.
7. Yamamoto, G. J. Mol. Struct. **1985**, 126, 413–420.
8. a) Yamamoto, G.; Ōki, M. Bull. Chem. Soc. Jpn. **1985**, 58, 1953–1961. b) Yamamoto, G.; Ōki, M. Bull. Chem. Soc. Jpn. **1986**, 59, 3597–3603.
9. Johnson, C. E., Jr.; Bovey, F. A. J. Chem. Phys. **1958**, 1012–1014
10. Hansen, P. E. Progr. NMR Spectrosc. **1981**, 14, 175–296. Marshall, J. L. Carbon-Carbon and Carbon-Proton NMR Couplings; VCH, Florida, 1983.
11. Kleier, D. A.; Binsch, G. QCPE, No. 165.
12. Nachbar, R. B., Jr.; Hounshell, W. D.; Naman, V. A.; Wennerstrom, O.; Guenzi, A.; Mislow, K. J. Org. Chem., **1983**, 48, 1227–1232.
13. Nachbar, R. B., Jr.; Mislow, K. QCPE, No. 559.
14. Allinger, N. L.; Lii, J.-H. J. Comput. Chem. **1987**, 8, 1146–1153. Lii, J.-H.; Allinger, N. L. J. Am. Chem. Soc. **1989**, 111, 8576–8582.
15. Kawada, Y.; Iwamura, H. J. Am. Chem. Soc. **1983**, 105, 1449–1459. Iwamura, H.; Ito, T.; Ito, H.; Toriumi, K.; Kawada, Y.; Ōsawa, E.; Fujiyoshi, T.; Jaime, C. ibid. **1984**, 106, 4712–4717.
16. Barnett, E. de B.; Cook, J. W.; Wiltshire, J. L. J. Chem. Soc. **1927**, 1724–1732.
17. Theilacker, W.; Berger-Brose, U.; Beyer, K.-H. Chem. Ber. **1960**, 93, 1658–1681.